R. & M. No. 2664
(11,731)
A.R.C. Technical Report

MINISTRY OF SUPPLY

AERONAUTICAL RESEARCH COUNCIL
REPORTS AND MEMORANDA

Load Diffusion at an Interspar Opening: Theoretical Methods of Analysis Compared with Strain Measurements on a Large Wing

By

D. C. Allen, B.A.

LONDON: HER MAJESTY'S STATIONERY OFFICE
1952
PRICE 7*s* 6*d* NET

Load Diffusion at an Interspar Opening: Theoretical Methods of Analysis Compared with Strain Measurements on a Large Wing

By

D. C. ALLEN, B.A.

COMMUNICATED BY THE PRINCIPAL DIRECTOR OF SCIENTIFIC RESEARCH (AIR), MINISTRY OF SUPPLY

Reports and Memoranda No. 2664*

June, 1948

Summary.—The diffusion of load from spar flanges into skin and stringers near an opening was investigated experimentally in a large wing structure undergoing strength tests. A comparison of measured strains with those given by theoretical methods shows that in general the flange loads are represented with reasonable accuracy. Any theory, however, in which the chordwise rib at the edge of the opening is ignored gives shear stresses much greater than those measured. Allowance for the bending stiffness of this rib produces values of shear stress comparable with those obtained experimentally.

1. *Introduction*.—As the use of stress bearing skins in wing structures is increasing, large openings, such as those required for the retraction of undercarriages, are becoming a major factor in design. At such an opening the end loads due to bending may have to be carried entirely by one spar flange, whereas away from the opening a large part of them may be carried by the skin and stringers. Diffusion of load from the spar flanges to the skin and stringers must then be provided for.

The present report is concerned with an example of this problem. A large wing specimen had an undercarriage opening in the lower surface, and at some distance from the opening the skin and stringers carried two-thirds of the end load due to the bending moment whereas the spar flanges carried only one-third. During a series of structural tests the strains were investigated by means of electrical resistance strain gauges and particular attention was paid to the diffusion of tension from the front spar lower flange into the skin and stringers inboard of the undercarriage opening.

The information obtained in these tests is examined with two main objects. The first is to reveal the strength and efficiency of the particular structure; the second is to compare the strain values obtained by measurement with those obtained by various theoretical methods and thus to determine which of these methods is most accurate. The assumptions on which these theoretical solutions are based, and the ease of their application to specific problems, are reviewed in this report.

The consistency of the strain gauge results is indicated by the agreement between measured flange loads and an integration of the measured shear loads adjacent to the flange (Fig. 10). The absolute values of the strains can be checked by comparing the total measured shear load and

---

* R.A.E. Report Structures 30, received 23rd August, 1948.

(51765) A

bending moment at a wing section with that applied in the test, and this check is carried out in Appendix II. The measured values agree among themselves but correspond to loads between 80 per cent and 90 per cent of those applied.

2. *The Specimen and Tests.*—The strength tests on the specimen from which the information was obtained were done under static loads producing predominantly bending actions in the wing structure. The test specimen, which is more fully described in Appendix I, comprised only the box made up of the two wing spars and the structure between them. Spanwise end-loads were carried mainly by closely spaced Z-section stringers and the skins which they reinforced. The upper interspar surface was complete, but the lower skin had a large opening at the outboard end of the inner wing to accommodate the undercarriage. The light alloy skin inboard of the undercarriage opening was reinforced by light alloy gusset plates in the two corners.

Electrical resistance strain gauges were used to indicate the distribution of shear and end load in the inner wing, particularly in the neighbourhood of the undercarriage opening. These positions are indicated in Figs. 13 and 14. At 54 per cent of the load which it was intended that the structure should ultimately carry, the rivets attaching the bottom skin to the front spar bottom flange on the port wing failed in shear from the undercarriage bay inner rib to the side of the fuselage. After the test, it was found that the extension flange to the undercarriage rib bottom boom had fractured at its attachment to the front spar.

As a result of the information obtained from the strain measurements, the light alloy gussets were replaced by two thicknesses of steel sheet, with a corresponding strengthening of skin to flange attachments. This reinforcement was arranged so that the spar flange and the undercarriage rib boom were also considerably strengthened. Before re-testing many more strain gauges were concentrated in the region of the previous failure (positions are shown in Fig. 15) to indicate the distribution of end load in the flange and of shear stress in the skin and its reinforcing.

In the repeat test the entire structure withstood the desired loading condition and ultimately failed at some other place at 103 per cent.

3. *Theoretical Work on Diffusion Problems.*—Workers in this field have concentrated on a simple form of the problem that occurs with many complications in aircraft wings. The problem is basically that of determining the distribution of stress in a panel, stiffened with longitudinal stringers and transverse frames, to which concentrated end loads are applied by means of edge members (flanges), and in which the loads are reacted by a uniform distribution of stress at some distance from their point of application (as illustrated in Fig. 16, Appendix III).

To make the problem tractable, the cross-section of the skin and stringers is assumed not to vary along the span, while the edge members are regarded as having either constant section or constant stress. Argyris[1] has put forward a method which is formally capable of handling flanges with arbitrarily varying area, but the labour involved in a practical case is considerable.

The stiffened sheet has been considered by some writers as a series of discrete stringers joined by shear webs, in what can be called the 'finite stringer' method. In the earlier work[2], any large number of stringers led to a determinental equation of prohibitive degree, but this mathematical complexity has since been resolved by Argyris and Cox[3].

Others[4,5] have regarded the stringers as spread into a uniform sheet. The shear carrying capacity and end load capacity are then regarded as acting over different thicknesses. This method leads to a shear stress adjacent to the flange which is infinite in value. It has been shown[6] that an infinite shear stress is not the result of the stringer-sheet assumptions, as had previously been suggested, but arises theoretically in any case where a load is applied to a member attached to a sheet whose edge normal to the member is unrestrained and the structure is such that the member remains straight.

Attempts have been made to introduce some of the properties of the transverse members into the solution. One method extends the stringer-sheet conception to the transverse direction to account for the end load carrying capacity of the ribs. It is suggested[1] that for reasonably large numbers of stringers the maximum shear stresses will agree closely with those given by the finite stringer method, although the position of the peak will be displaced from the corner along the flange. An end member with finite stiffness under end load has been considered[5]. In the case which has been solved, in which the flange area is large compared with the total stringer area, an infinite value for the corner shear stress is again obtained and the results agree roughly with those obtained by stringer-sheet assumptions disregarding the end member. But if the stiffness of the end member in bending in the plane of the sheet is considered, as distinct from its stiffness under end load, a marked redistribution of shear stress takes place. A finite value for the peak shear stress is obtained, even though the stringer-sheet approximations are made[7].

All the methods surveyed lead to distributions of flange load which agree closely among themselves except at very small distances from the point of application of the load. These distributions are conveniently displayed in the Royal Aeronautical Society Data Sheet[8] (Number 02.05.11), which is based on the work already referred to[1,2,4], and which can be used directly to determine the rate of diffusion of the flange load. The shear stress adjacent to the flange depends critically on the exact shape of the end load distribution curve. Methods which disregard the properties of the end member lead to a peak shear stress which increases rapidly with the number of stringers, and becomes infinite in the limiting case of a stringer-sheet, a result which is clearly of little use to a designer.

4. *Application of Theoretical Methods to the Test Structure.*—The distribution of stress can be calculated, in accordance with the assumptions, for the simple theoretical structure discussed in section 3. Before the values so obtained can be compared with measurements on the actual structure, they must be changed to allow for various differences between the actual structure and the simple theoretical one. Of these differences the following are likely to have the greatest effect and they will be considered in turn :—

(a) The flange area is neither constant spanwise nor sufficiently tapered to give constant stress.

(b) The geometry and loading of the structure are asymmetrical.

(c) Local relief and redistribution of stresses is afforded by discrete rivets, by the slip of rivets and by yielding and buckling of materials.

(d) Reinforcing plates give local assistance to the skin.

(e) The stiffness and degree of end fixity of the chordwise rib boom are difficult to estimate.

4.1. The area of the lower front spar flange, omitting the addition provided by attached plating and the reduction due to rivet and bolt holes, is shown in Fig. 3. A curve showing the variation of area required to maintain constant stress in the flange as deduced from the finite stringer assumptions for a particular arrangement of stringers and sheet is also included. It will be seen that, even over a length equal to the inter-spar distance, the actual variation is small compared with that for the extreme case of the flange tapered to give constant stress. In the subsequent analysis the flange is regarded as having a constant area equal to that which it has at the opening. An approximate allowance for the reduction in area which does occur is included in the final distribution of shear stress.

4.2. The rear spar flange is not exactly equal in area to the front spar; it is attached to a plate web and it tapers more rapidly; the shear reinforcing is not symmetrically distributed; the loads carried by the front spar flange are greater than those carried by the rear spar in the ratio of about 1·7 to 1. The case of a panel with two unequal flanges and unequal loads applied to them has been treated in Ref. 5, and the distributions of load in the flanges obtained in that paper for a particular example are compared in Appendix III with the distributions in the two symmetrical panels derived from separate parts of the original panel. The distribution of flange loads in the symmetrical panels, which are derived from the original panel on the basis of equal diffusion loads, approach closely those for the original asymmetric panel even for a case in which the larger flange area is as much as four times the small flange area. Hence, the front spar flange and adjacent panel of the actual wing will be regarded as part of a symmetrical panel in which the flange load to be diffused is the same as that in the actual wing panel.

4.3. The theoretical consideration of the localised effects introduced by riveting is a task of too great a magnitude in comparison with its practical value to justify its being undertaken. For the panels adjacent to the front spar flange the buckling stress under shear loads is well above the ultimate shear stress for the material and therefore no account will be taken of buckling of panels.

4.4. Analysis of diffusion problems is, in the main, restricted to cases where the sheet thickness does not vary either in the spanwise or chordwise directions. Small reinforcing plates introduced in areas of highest shear stress will serve to reduce the shear stress at the expense of some increase in shear per unit length over a localised area. Large reinforcing plates have an effect equivalent to an increase in skin thickness over the whole of the panel, since the local diffusion at the edges of the plate will not spread far into the plate. It is difficult to lay down rules for estimating the effect of reinforcing plates, and analytical work even when the problem is very much simplified is prohibitive and tends to lead to values of shear stress which are unreasonably large. In the particular case of the reinforcement provided in the wing under test, two equivalent thicknesses have been considered and the results compared with each other and with those obtained by measurement.

4.5. The spanwise bending stiffness of the rib boom, whose section is shown in Fig. 4, can be regarded as having any value within the range $0 \cdot 1 \times 10^7$ lb/sq in. to $2 \cdot 5 \times 10^7$ lb/sq in. according to the amount of the free flange that is considered to be effective. Mansfield[7] gives the maximum shear stress, when typical flange and sheet areas are taken, as ranging from $0 \cdot 56$ to $0 \cdot 35$ times the maximum flange stress for this range of values of rib stiffness. This means that if the minimum rib stiffness were used for design, it would be possible in this case to over-estimate the shear stresses by anything up to 60 per cent.

5. *Presentation of Theoretical and Experimental Results.*—From the point of view of the designer, the important quantities in the diffusion problem are the flange load and the shear stress adjacent to the flange. These quantities are evaluated, according to the various theories, for the wing in both its unmodified and modified condition.

5.1. *Unmodified Wing.*—The relevant sizes at section $259 \cdot 5$ are given in Appendix I.

Ordinary bending theory gives the stress in the front spar flange at section $259 \cdot 5$ as 54,500 lb/sq in. The effective area of the flange, allowing for the 4-in. width of skin and reinforcement attached, is $2 \cdot 44$ sq in. The flange load is, therefore, 133,000 lb. This assumes that the spanwise change of load in the front spar is linear and so does not allow for the sudden increases of load caused by the front spar bracing. The theoretical value of the shear load in the front spar is 680 lb/in., which is equivalent to an increase of tension in the front spar flange of 20,400 lb at a node of the bracing, one of which occurs at section $259 \cdot 5$. The value of the load given by ordinary bending theory should be increased by about one half of this figure to give the actual flange load at the seciton $259 \cdot 5$, which will be taken as 143,000 lb.

Theoretical results will be based on the diffusion of this flange load of 143,000 lb into symmetrical panels, with section uniform chordwise and constant spanwise; the dimensions of one (A) are calculated on the assumption that the reinforcing plates are not present; and of the other (B) on the assumption that the reinforcing plate is sufficiently extensive to be regarded as equivalent to a uniform increase of sheet thickness.

The geometrical properties on which the rate of diffusion depends are contained in three parameters; α, k, μ; defined by

$$\alpha = F/at_s$$

$$k^2 = Et_s/Gt$$

$$\mu = \frac{1}{a}\sqrt{\left(\frac{Gt}{Et_s}\right)}$$

where F is the effective flange area,

a is half the width of the panel,

t is the thickness of the sheet in shear,

t_s is the stringer-sheet thickness,

G and E are the elastic moduli for the material.

The values of these parameters appropriate to the two panels and based on the dimensions given in Table 6 are:

	A	B
α	0·965	0·66
k^2	4·26	3·33
μ in.$^{-1}$	0·0143	0·0161

To compute flange loads and shear stresses it is necessary to include a value for the length (l) of the panel. The length to the centre-line of the wing is 259·5 in. For sufficiently large values, a change in l will not make any appreciable difference to the stresses at the opening. In Ref. 4, the minimum value of l for the end conditions not to affect the stresses at the opening is given as $1 \cdot 5a$. For convenience of applying the Data Sheet results, a value of l to give $\mu l = 2$ will be chosen, *i.e.*, $l = 140$ in. for panel A and 124 in. for panel B.

Flange loads and shear per unit length adjacent to the flange have been determined from available theories as set out in the Data Sheets and elsewhere and are shown in Figs. 6 and 7. When the bending stiffness of the rib boom is taken into account, it is possible to obtain accurately the size of the maximum shear stress from the curves given in R. & M. 2663[7]. The spanwise position at which this maximum occurs and the distribution of shear stress leading up to it can be assessed approximately. Lines showing the value of the peak shear per unit length and its approximate position are included in Fig. 7.

A few points of measured flange stress are available, as shown in Table 2, and a number of sections of shear stress (Table 1). Fig. 5 shows chordwise plots of measured shear per inch; the results of extending these curves to the front spar flange are included in Fig. 7 for comparison with the theoretical values.

5.2. *Modified Wing*.—The dimensions of the skin and its reinforcement after modification are given in Appendix I.

Simple bending theory gives the modified stress in the flange as 43,700 lb/sq in., or the load as 124,000 lb, to which must be added 10,000 lb due to the front spar bracing, giving a total load of 134,000 lb.

The symmetrical panel considered is one in which the larger reinforcement continues over the whole sheet and the smaller plate is neglected as far as its contribution to altering the shear loads is concerned. The dimensions of this panel (C) given in Table 6 lead to values of the diffusion parameters of:

α	0·545
k^2	2·96
μ	0·0171 in.$^{-1}$.

To give $\mu l = 2$, l can be taken as 117 in.

Curves of flange load and shear per unit length are contained in Figs. 10 and 11, which also show experimental results based on the values of Tables 3 and 4 and the plots of Figs. 8 and 9.

6. *The Strength of the Structure.*—6.1. *The Unmodified Wing.*—The curves of shear load given in Fig. 7 and their relation to measured loads suggest that the maximum shear occurring in the panel is approximately that given when allowance is made for the root rib stiffness and the reinforcement is regarded as producing an equivalent uniform increase of skin thickness. This value of shear load, *i.e.*, 2,870 lb/in. at 100 per cent load, will be used to estimate the strength of the sheet and its attachment to the flange.

The spacing of rivets at the corner was 4 × 5/32 in. rivets/in. which, allowing 410 lb per rivet, gives a failing load of 1,640 lb/in., corresponding to 57 per cent load. (Failure of the riveting took place in the test at 54 per cent load.)

The sheet was loaded in a combination of tension and shear along the line of attachment to the flange. A relation between the allowable shear stress and the tensile stress at the line of attachment, each considered in terms of the specified ultimate stress of the material, is displayed in Data Sheet Number 02.03.17. The sheet material D.T.D. 546 has a specified ultimate stress of 27 tons/sq in. A process of successive approximation leads to an estimated failing load for the sheet of 72 per cent.

6.2. *The Modified Wing.*—On the same basis, the maximum shear load in the modified wing is estimated as 3,360 lb/in. at 100 per cent load. The attachment consisted of 2 B.A. high tensile steel bolts at a spacing of 6/in. An allowed strength of 2,000 lb per bolt gives a failing load of 12,000 lb/in.

To estimate the sheet failing load, it will be assumed that the distribution of load between the sheets remains in the ratio of their thicknesses times Young's modulus, even when yielding has occurred. Tensile tests on the steel reinforcing sheet (specified as D.T.D. 166B) gave an ultimate tensile stress of 82 tons per sq/in. and an E of 25×10^6 lb/per sq in. The failing stress of the equivalent light alloy sheet is then $32 \cdot 8$ tons/sq in., which is greater than the ultimate stress for D.T.D. 546. This latter stress must therefore be taken to give the failing load of the sheet. The equivalent thickness in light alloy is $0 \cdot 191$ in.; the shear stress at 100 per cent load is therefore 17,500 lb/sq in. The failing lead estimated from the Data Sheet is 107 per cent load.

The specified figures for the properties of D.T.D. 166B are 52 tons/sq in. for the ultimate stress and $28 \cdot 5 \times 10^6$ lb/sq in. for E. The equivalent light alloy failing stress is then $18 \cdot 3$ tons/sq in. The shear stress and flange stress will be slightly reduced as a result of the increase in E of the material. If these reductions are neglected, the sheet is estimated to reach its failing load at only 74 per cent load.

The importance in this low figure lies in the difficulty of satisfying the requirements for proof load, namely that the $0 \cdot 1$ per cent proof stress should not be exceeded at that load. After yield has taken place, the load will be redistributed between the plates, and the fraction of load diffused from the flange will be reduced. For a flange of constant section this fact will not have to be considered in relation to the flange stresses, but will lead to a welcome increase in the load necessary to cause failure of the sheet.

7. *Consideration of Results and their Use in Design.*—7.1. *Spar Flange Loads.*—The theoretical distributions of flange load given by the finite stringer method and the approximate stringer-sheet method agree closely at the higher values, and the exact stringer-sheet theory gives a more rapid reduction of flange load at the root. In both conditions of the wing, the measured distribution of load agrees in shape with the distribution given by the finite stringer theory but is smaller in magnitude by a fixed amount (about 10 per cent of the root load). No allowance has been made in the theoretical curves for the amount of load distributed to the stringers by the root rib, but calculations in some representative cases indicate that this would be of the order of 10 per cent of the root load.

The calculated value of the spar flange stress at the opening does not depend on the particular theory chosen for determining the diffusion stresses. The stress in the flange drops rapidly as the distance from the opening increases and it is not likely in practice that the flange will be tapered so much that this stress is critical, since severe tapering increases the shear stresses in the skin. The shear stress adjacent to the flange depends only on the change of load in the flange, and it appears that the distribution is reasonably represented by the finite stringer theory.

7.2. *Shear Stresses in Skin.*—The theoretical distributions of shear load resulting from the use of the finite-stringer method of analysis give a very large maximum shear load at the corners of the panel, and this peak increases if the number of stringers is increased. In the modified wing test, sufficient readings of shear stress were obtained to indicate that the shear stress does not in fact continue to increase more and more rapidly towards the corner; considerations of failing loads show that no such high peaks of shear stress can have occurred.

When the bending stiffness of the rib boom is taken into account, the calculated maximum shear stress is very much smaller than that given by the finite-stringer method (only $0 \cdot 52$ times that value for the modified wing) but still exceeds the values of shear stress as measured. Estimates of the shear stress distribution for the case of a constant area flange can be based on the curves given by Mansfield[7]. The maximum value for a chosen rib boom stiffness can be determined exactly: the position of the peak value and the curves leading to this peak can be drawn approximately. This is done in Fig. 11, and the curves agree well with the measured values at the peak. At a point 10 in. from the opening the flange area is reduced and successive reductions take place at points further along. The effect of this reduction can be estimated by comparing the reduction in area with that necessary to give constant flange stress and introducing a comparable increase in shear stress. Such a procedure will be at best only approximate. Its use can be justified on the ground that the peak shear stress will be accurately assessed and only the smaller shear loads will be subject to error; these will in any case be included within a range bounded on the lower side by the values for the constant-area flange and on the upper by those for the constant stress flange.

A considerable increase in the bending stiffness of the rib boom does not much reduce the peak shear stresses. An increase in the size of the edge flange and hence a reduction of its stress may be a profitable way to increase the strength of a structure (or to reduce its weight to the optimum) since a reduction of the root tensile stress means an increase in the allowable shear stress in the sheet, which in turn means a reduction in the thickness of sheet necessary. As a rough guide, an increase of sheet thickness from t to k^2t leads to a reduction in shear stress to k^{-1} times its original value or to an increase of shear load per unit length to k times its original value.

The question of the most economical way to achieve a given strength in a diffusion panel will not be pursued in this report.

8. *Conclusions.*—Stresses deduced from static strain measurements taken in the neighbourhood of the undercarriage opening of a large wing specimen have been compared with those calculated by various simplified theories. The distribution of end load in the flange is reasonably represented by any of the theories. At the edge of the opening the maximum shear stress in the sheet, as estimated without allowing for the bending stiffness of the chordwise rib, is greatly in excess of the measured values. If a minimum value of the rib stiffness is used the estimated maximum shear stress is slightly higher than the greatest measured value. To get accurate estimates of load distribution away from the opening allowance must be made for variation of the flange area.

REFERENCES

No.	Author	Title, etc.
1	J. Hadji-Argyris	Diffusion of Symmetrical Loads into Stiffened Parallel Panels with Constant Area Edge Numbers. R. & M. 2038. November, 1944.
2	H. L. Cox	Diffusion of Concentrated Loads into Monocoque Structures III. R. & M. 1860. September, 1938.
3	J. Hadji-Argyris and H. L. Cox	Diffusion of Load into Flat Stiffened Panels of Varying Cross-Section. R. & M. 1969. May, 1944.
4	M. Fine and H. G. Hopkins ..	Stress Diffusion Adjacent to Gaps in the Interspar Skin of a Stressed-Skin Wing. A.R.C. Report No. 5941. May, 1942. (To be published.)
5	W. J. Goodey	Stress Diffusion Problems. *Aircraft Engineering*. June-November, 1946.
6	E. H. Mansfield	Diffusion of Load into a Semi-Infinite Sheet—Part I. A.R.C. Report No. 11,268. November, 1947. (To be published.)
7	E. H. Mansfield	The Effect of Spanwise Rib-boom Stiffness on the Stress Distribution near Wing Cut-Out. R. & M. 2663. December, 1947.
8	—	Royal Aeronautical Society Data Sheets on Stressed Skin Structures. Revised to December, 1946.

APPENDIX I

A Short Description of the Specimen, giving Relevant Dimensions and Test Loads

The test wing was full span except for omission of wing tips, but in the chordwise direction comprised only front and rear spars and the structure between them. The wing was made in three sections: an inner wing 603 in. span designed to carry the fuselage, engines and airscrews and undercarriages; and two outer wings each 354 in. span incorporating the fuel tanks in the inboard 145·5 in. of their span. Inner-wing sections are referred to by their measurements from the fuselage centre line and outer-wing sections by their measurements from the wing joint, 301·5 in. from the fuselage centre line. A length of parallel circular fuselage, 100 in. in diameter and 40 ft 5 in. long, was attached to the wing for holding it in the test frame.

Spanwise end loads were carried mainly by the closely spaced Z-section stringers and the skins which they reinforce. The spar booms were relatively light extrusions. The upper interspar surface was complete, but the lower surface of the inner wing was cut away between 259·5 in. and 301·5 in. from the fuselage centre line to accommodate the undercarriage, and at this opening the end-loads were taken by reinforcing the front spar bottom flange and adding a longeron at the rear.

The front spar of the inner wing (at 27 per cent chord) was a braced structure from 55·5 in. to the joint at 301·5 in. The rear spar had a complete plate web with vertical stiffeners. There was an additional plate web at 15 per cent chord from 259·5 in. to 301·5 in.

The ribs of the inner wing were spaced at about 18 in. pitch and ordinarily consisted of rolled Z-section light alloy booms braced by light alloy tubes. Rib 259·5 at the inboard end of the undercarriage cut-out had a diaphragm web and extruded booms with heavy teeth extending between stringers to form a shear attachment to the skin. Fittings for the undercarriage were carried on heavy vertical stiffeners attached to the rib just forward of the rear spar.

The specimen was anchored by the ends of the fuselage section with the datum line $\frac{1}{2}$ deg nose down; vertical loads were applied at points on the spars. The ultimate fully factored design loads are called 100 per cent loads. The positions of the applications of these loads are shown in Fig. 1 and their values are listed in Table 5. Shear, bending moment and torque diagrams corresponding to the 100 per cent loads appear in Fig. 2.

Detailed measurements of material sizes were made by the manufacturers while the specimen was being built: analytical work in this report is based on these measurements.

Specimen as originally tested.—The relevant sizes at section 259·5 in. are:

Flange areas	Front spar lower flange	2·27 sq in.
	Rear spar lower flange	2·17 sq in.
Stringer area		0·074 sq in.
Distance between spar datum lines		70·5 in.
Stringer pitch		2·2 in.
Skin thicknesses:		
2 in. forward to 22 in. aft of front spar datum ..		0·041 in.
22 to 46 in. of front spar datum		0·045 in.
46 to 70·5 in. of front spar datum		0·050 in.

Front spar reinforcing plate extends from 2 in. forward to 21·5 in. aft of front spar datum and has thickness 0·041 in.

Rear spar reinforcing plate extends from rear spar datum 10·95 in. forward and has thickness 0·050 in.

All skins and reinforcing plates are made in material to specification D.T.D. 546.

To allow for the presence of rivet holes in the tension members an effective area of 0·94 the actual area is used for all such members.

Specimen as tested after modification.—The dimensions altered as a result of the modifications are:

Front skin panel thickness	0·064 in.
Front spar reinforcing plates extending from—	
(1) 2 in. forward to 19 in. aft of front spar datum thickness	0·026 in.
(2) 2 in. forward to 10 in. aft of front spar datum thickness	0·025 in.

Both made from material to specification D.T.D. 166B.

Rear spar reinforcing plates are similar.

APPENDIX II

A Comparison of Measured and Applied Actions

A useful check on the strain measurements is provided by computing from them the total actions (shear forces, torque and bending moments) at a convenient section, for comparison with the known applied actions.

In the tests on the unmodified wing, measurements of shear strain were made at a number of sections of the wing and measurements of axial load were made at a few sections. In the modified version, complete section measurements were reduced to two of shear and one of axial load.

For each condition of the wing, an estimate has been made of the measured vertical shear load and of the bending moment about the section datum for one section (250) of the wing.

The results tabulated below show good agreement between themselves, but are all considerably lower than the applied values. At the section at which the estimates have to be made there are rapid rates of change of stress, since diffusion from the opening is incomplete, and this may mean that undue weight has to be given to a few of the strain readings with a resulting loss of accuracy in the final sum.

Section 250

Vertical Shear Load in lb as deduced from strain readings

	Unmodified wing	*Modified wing*
Rear Spar Web	5,800	4,960
Bottom Skin	3,770	4,440
Top Skin	3,320	2,940
Front Spar Bracing	18,200	16,200
End load in Front Spar Flanges : Lower ..	480	440
Upper ..	380	380
Total	31,950	29,360
Fraction of Applied Vertical Shear Load (36,500 lb)	0·88	0·81

Bending Moment about Section Datum in lb/in. as deduced from Strain Readings

		Load	*Moment*	*Load*	*Moment*
Top	Front spar flange	— 39,100	830,000	— 38,400	815,000
	Skin and stringers	— 145,100	2,994,000	— 141,100	2,889,000
	Rear spar flange	— 6,700	80,000	— 7,200	110,000
Bottom	Front spar flange	84,600	939,000	84,100	933,000
	Skin and stringers	71,400	726,000	96,900	922,000
	Rear spar flange	37,400	185,000	36,400	180,000
Front spar bracing		— 10,200	54,000	— 9,100	48,000
	Total	193,400 — 201,100	5,808,000	217,400 — 196,500	5,898,000
Fraction of applied bending moment (6,600,000 lb/in.)			0·88		0·90

APPENDIX III

A Comparison Between the Flange Loads in an Asymmetrical Panel and those in Two Symmetrical Panels

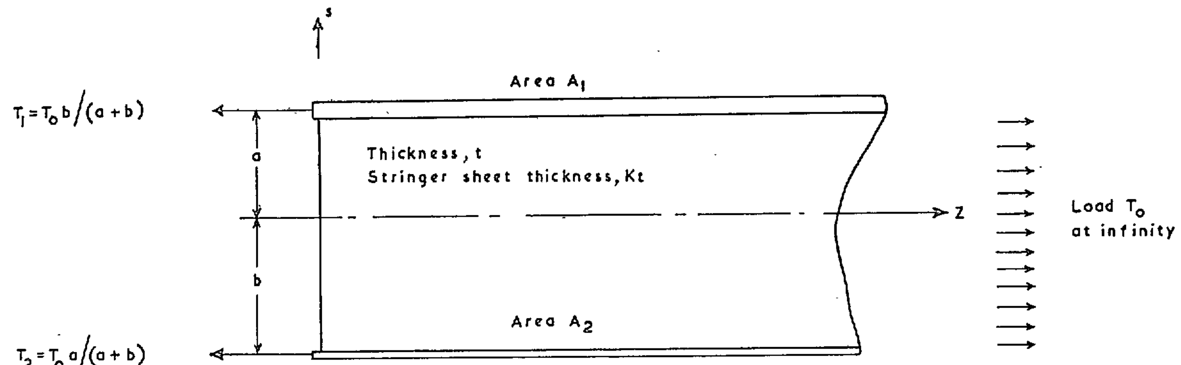

Figure 16a

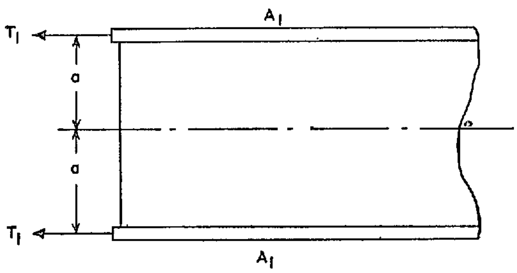

Figure 16 b

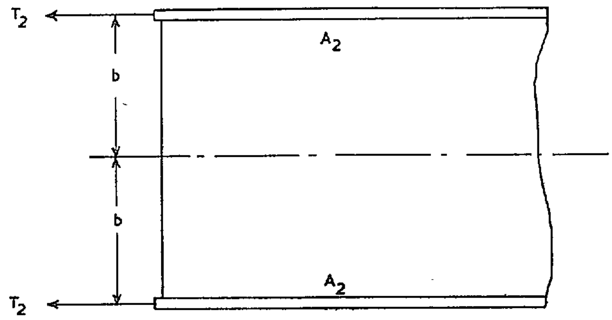

Figure 16c

A numerical example of the case shown in Fig. 16a has been worked out in Ref. 5 for the following values of the panel dimensions

Larger flange area, A_1	2·5 sq in.
Smaller flange area, A_2	0·6 sq in.
Stringer sheet thickness, Kt	0·0644 in.
K	4/3
Centroid of applied loads given by	
a	21·8 in.
b	38·2 in.
$m_1 = A_1/aKt$	1·786
$m_2 = A_2/bKt$	0·244

The distributions of load in the two flanges are reproduced in Fig. 12 (curves A, a). The figure also shows for comparison the flange loads (curves B, b) in the two symmetrical panels whose two halves together make up the original panel. The panels are sketched in Figs. 16b and c. The greatest difference occurring is about 7 per cent of the root flange load.

If the panel is divided so that the loads to be diffused from the flanges are the same in the derived panel as in the original symmetrical panel, improved agreement is obtained (curves C, c; the greatest difference is 4 per cent of the root load.

TABLE 1

Unmodified Wing Shear Loads at 100 *per cent Load in lb/in.*

Positions are shown in Figs. 13 and 14.

Section	270		250		238		199	
	No.	Shear	No.	Shear	No.	Shear	No.	Shear
Bottom Skin	152	−256	162	−1,680	211	−1,364	236	−508
	153	−614	164	−715	212	−829	238	−492
			166	−306	213	−367	242	−328
			168	22	214	0	244	0
			172	300	215	367	246	241
			174	536	216	680	248	320
			176	844	217	792	312	576
	131	296	178	1,176	218	936	314	600
Rear Spar Web	132	—	183	330	221	288	317	314
	133	684	184	302	222	302	318	314
	134	684	185	—	223	302	321	363
Top Skin	135	389	188	402	224	352	324	353
	136	233	192	146	225	388	326	292
	137	138	194	292	226	338	328	292
	138	138	196	133	227	297	332	256
	141	56	198	51	228	133	334	82
	142	−125	202	−51	231	−51	336	−148
	143	−251	204	−289	232	−263	338	−165
	144	−372	206	−547	233	−289	342	−314
	145	−424						
	146	−128						
Front Spar	147	168						
	148	192						
	151	128						

TABLE 2

Unmodified Wing End Load Stresses at 100 per cent Load in lb/sq in.

Positions are shown in Figs. 13 and 14.

Section 250

	Front Spar Lower Flange		Bottom Skin							Rear Spar Flanges
Gauge	158	161	163	165	167	171	173	175	177	181
Stress	34,000	40,400	7,600	9,600	4,400	3,800	9,000	4,400	5,800	17,200
	Rear Spar Flanges			Top Skin						
Gauge	182	186	187	191	193	195	197	201	203	205
Stress	19,800	—	—7,600	—7,600	—10,800	—16,000	—19,800	—22,400	—13,400	—24,000
	Front Spar Upper Flange									
Gauge	207	208								
Stress	—23,000	—21,200								

Section 199

	Front Spar Lower Flange		Bottom Skin							Rear Spar Flanges
Gauge	234	235	237	241	243	245	247	311	313	315
Stress	39,600	36,400	40,400	29,400	26,800	26,800	25,000	17,400	30,000	21,800
	Rear Spar Flanges			Top Skin						
Gauge	316	322	323	325	327	331	333	335	337	341
Stress	16,000	—8,400	—8,400	—13,400	—25,000	—18,600	—13,400	—21,600	—25,000	—25,600
	Front Spar Upper Flange									
Gauge	343	344								
Stress	—16,000	—16,000								

TABLE 2—*continued*

Front Spar Tubes

Gauge ..	774	777	782	783	785	786	793	794
Strain × 10^6	−1,020	3,340	2,800	−2,260	−1,460	2,320	−1,740	2,120
Area ..	0·314	0·314	0·314	0·314	0·196	0·314	0·402	0·402
$E \times 10^{-3}$ ..	29·5	29·5	29·5	29·5	10	29·5	29·5	29·5
Load ..	−9,450	31,000	26,000	−20,900	−2,860	21,500	−20,650	25,180

TABLE 3

Modified Wing Shear Loads at 100 per cent Load in lb/in.

Positions are shown in Fig. 15.

Section	270		256		253		250		245		238		236		227		201	
	No.	Shear	No.	Shear	No.	Shear	No.	Shear	No.	Shear	No.	Shear	No.	Shear	No.	Shear	No.	Shear
Bottom Skin	152	−211																
	153	−552																
			941	−2,390	945	−2,257	947	−2,270	963	−1,929					965	−1,128	966	−671
			942	−1,831	946	−1,993	948	−1,917					964	−1,279				
			943	− 883			961	−1,357										
			944	− 645			962	− 893					212	− 835				
							166	− 257			213	−385						
							186	34			214	20						
							172	311			215	331						
							174	592			216	712						
							176	1,035			217	1,012						
							178	1,459			218	1,173						
Rear Spar	132	—					183	—			221	262						
	133	656					184	273			222	240						
	134	650					185	263			223	217						
Top Skin	135	336					188	358			224	329						
	136	264					192	312			225	358						
	137	168					194	302			226	309						
	138	161					196	115			227	221						
	141	—					198	58			228	163						
	142	− 81					202	− 67			231	− 67						
	143	−195					204	−281			232	−255						
	144	−430					206	−504			233	−615						
	145	−420																
	146	−120																
Front Spar	147	144																
	148	150																
	151	120																

TABLE 4

Modified Wing End Load Stresses at 100 *per cent Load*

Positions are shown in Figs. 13, 14 and 15.

Section		Front Spar Lower Boom					
		253	250	245	236	227	201
Front Flange	Top	36,700	32,200	30,700	24,700	15,400	38,600
	Centre	34,800	31,500	28,800	24,400	—	32,200
Rear Flange	Top	31,500	27,700	28,100	25,100	14,600	36,000
	Centre	31,800	26,900	25,800	23,600	16,500	31,800

Gauge Position	Front Spar Tubes							
	774	777	782	783	785	786	793	794
Strain $\times 10^6$	− 2,220	2,810	2,640	− 2,020	− 1,580	1,880	− 1,750	1,880
Area ..	0·314	0·314	0·314	0·314	0·196	0·314	0·402	0·402
Load ..	−20,570	26,030	24,450	−18,650	− 3,100	17,400	−20,850	22,250

Section 250

Inner Wing Compression Surface

	Rear Spar Flange		Top Skin							Front Spar Flange	
Gauge ..	186	187	191	193	195	197	201	203	205	207	208
Stress ..	−5,600	−9,000	−7,900	−13,900	−13,900	−18,800	−19,500	−12,700	−22,100	−24,000	−19,500

TABLE 5

Loading Table.—All loads 100 per cent loads in lb; positive loads upwards; negative loads downwards. For positions of loading stations, *see* Fig. 1.

1. *Spar Loads*

	Loading station Rib positions	Port Wing		Starboard Wing	
		Front Spar	Rear Spar	Front Spar	Rear Spar
Inner Wing	55·5	+4,375	− 375	+4,375	− 375
	106·5	−3,550	+1,700	−3,550	+1,700
	121·5	−3,493	+1,685	−4,250	+1,102
	157·5	+6,027	0	+5,250	− 343
	208·5	−1,650	+ 628	−1,650	+ 598
	223·5	−1,637	+ 587	−1,637	+ 587
	259·5	+3,948	− 748	+3,948	− 748
Outer Wing	301·5	+4,703	+1,097	+4,703	+1,097
	0				
	72	+8,200	0	+7,000	− 490
	145·5	+4,675	+3,465	+3,566	+2,950
	220·5	+4,660	0	+4,660	0
	282	+2,777	− 177	+2,777	− 177
	354	+2,448	+1,452	+2,448	+1,452

2. *Rib Loads.*—Applied to starboard wing only. All loads positive.

Rib 138·75 (Inner Wing)	Dist. forward of T.E. in.	58·45	70·15	85·0	96·7	110·85	121·45		
	Load lb	200	200	455	455	590	590		
Rib 108 (Outer Wing)	Dist. forward of T.E. in.	47·2	55·35	65·55	73·3	83·9	92·6	102·7	109·8
	Load lb	215	215	400	400	590	590	452	452

TABLE 6

Panel Dimensions

	A	B	C
Effective flange area, F, sq in. . .	2·29	2·44	2·84
Effective stringer area A, sq in. . .	0·154	0·239	0·336
Stringer sheet thickness t_s, in. . .	0·070	0·109	0·153
Shear sheet thickness t, in.	0·041	0·082	0·129*
Number of stringers n		30	
Width of panel $2a$, in.		68	
Stringer pitch b, in.		2·2	
$\alpha = F/at_s$	0·965	0·66	0·545
$k^2 = Et_s/Gt$	4·26	3·33	2·96
$\mu = \frac{1}{a}\sqrt{\left(\frac{Gt}{Et_s}\right)}$ in.$^{-1}$	0·0143	0·0161	0·0171

* This figure is an equivalent thickness in light alloy taking E for the steel as 25×10^6 lb/sq in. This low value of E was obtained on control tests from the material used in the wing.

(51765)

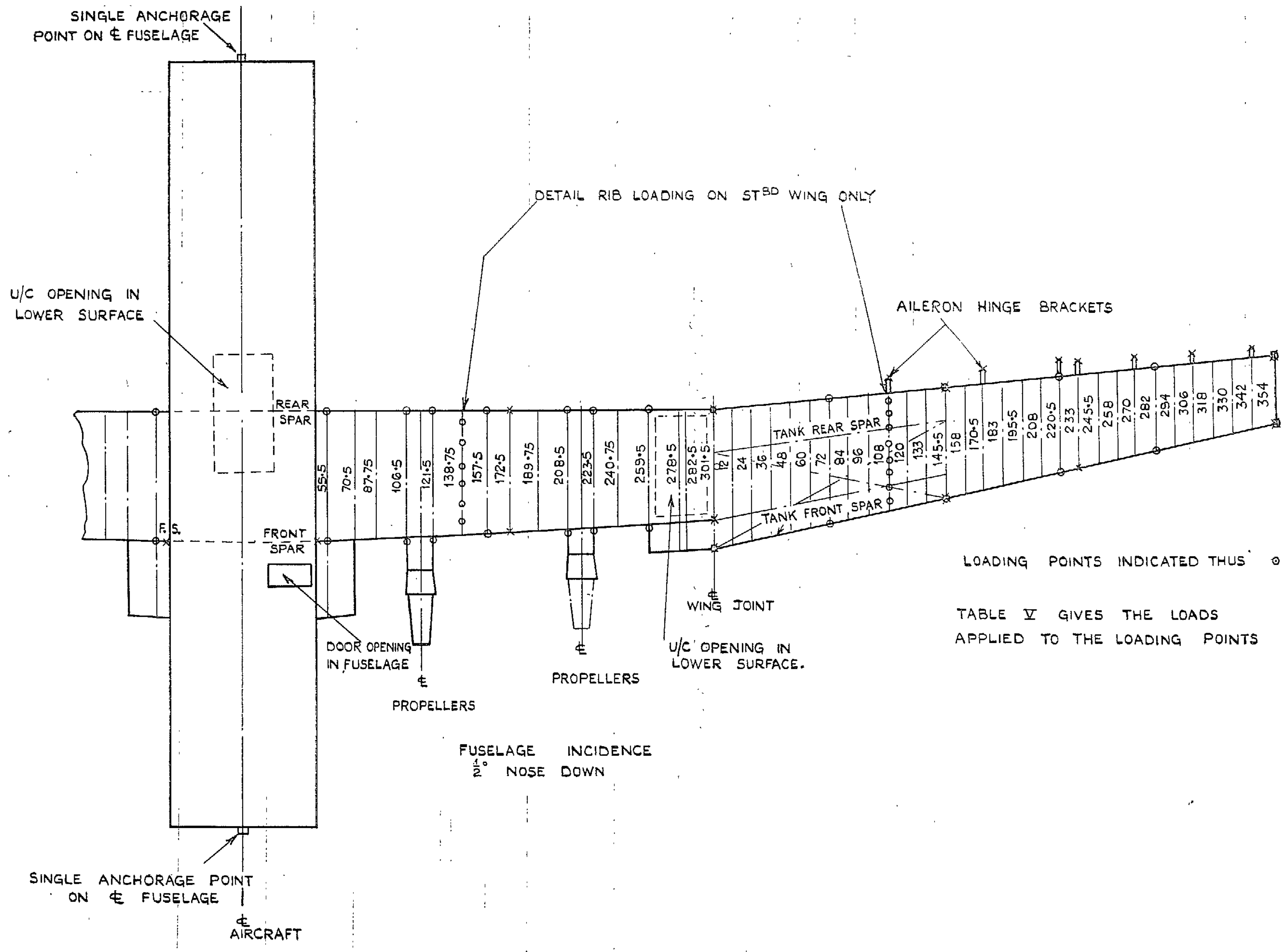

FIG. 1. Diagram of specimen and loading positions.

B

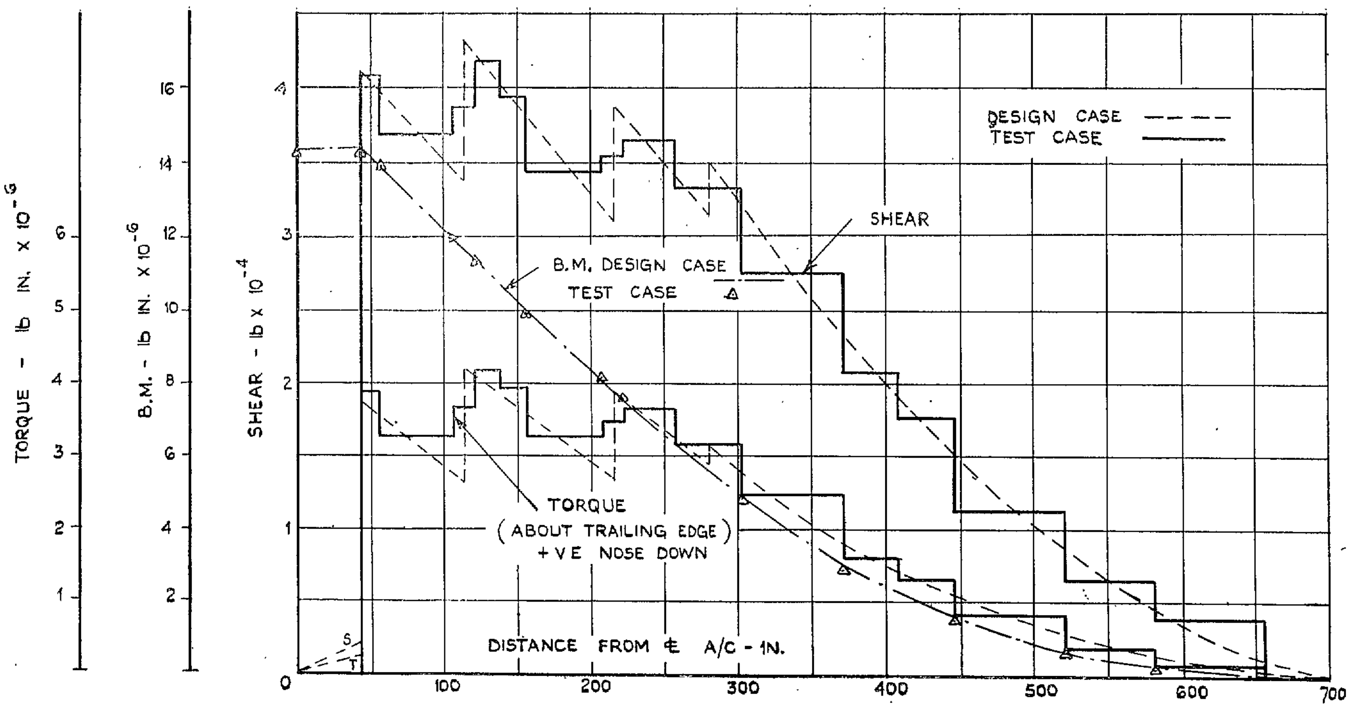

FIG. 2. Shear, bending moment and torque diagrams.

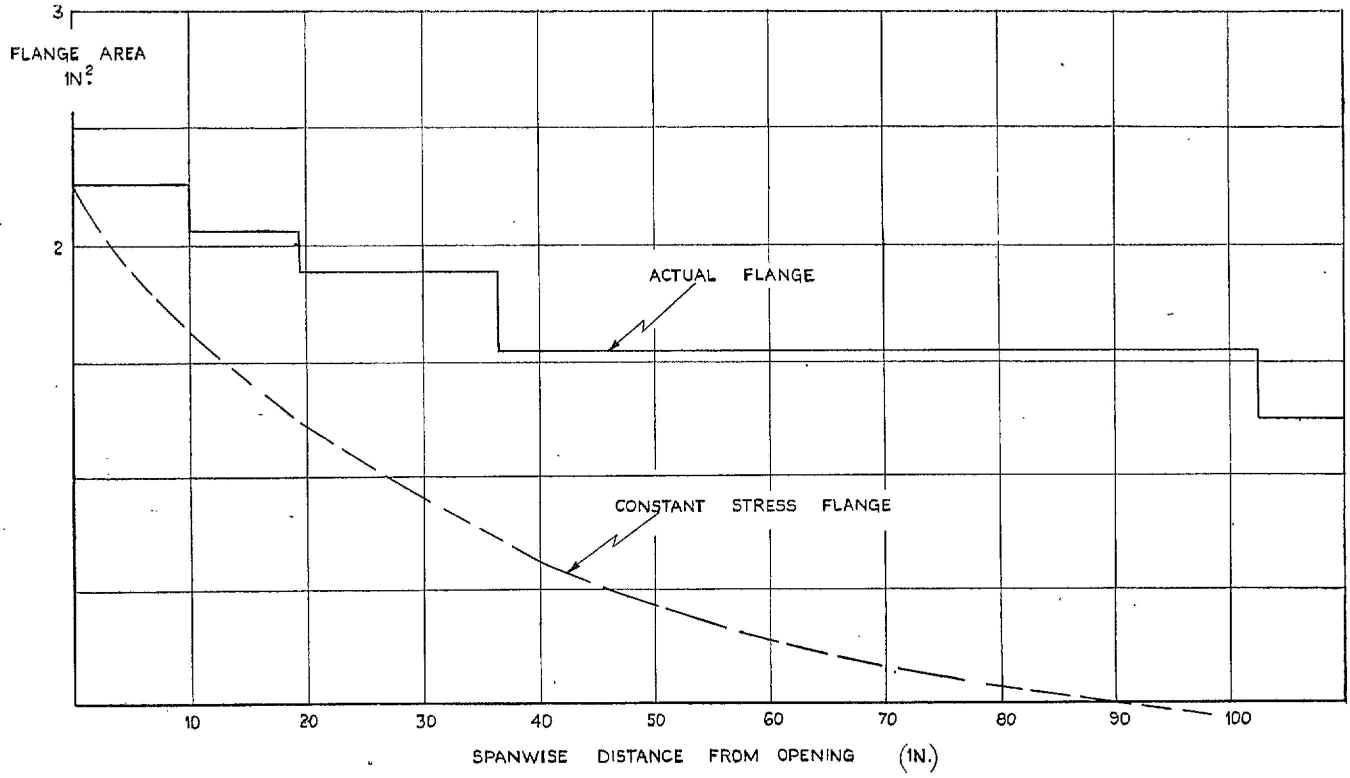

FIG. 3. Front spar flange area.

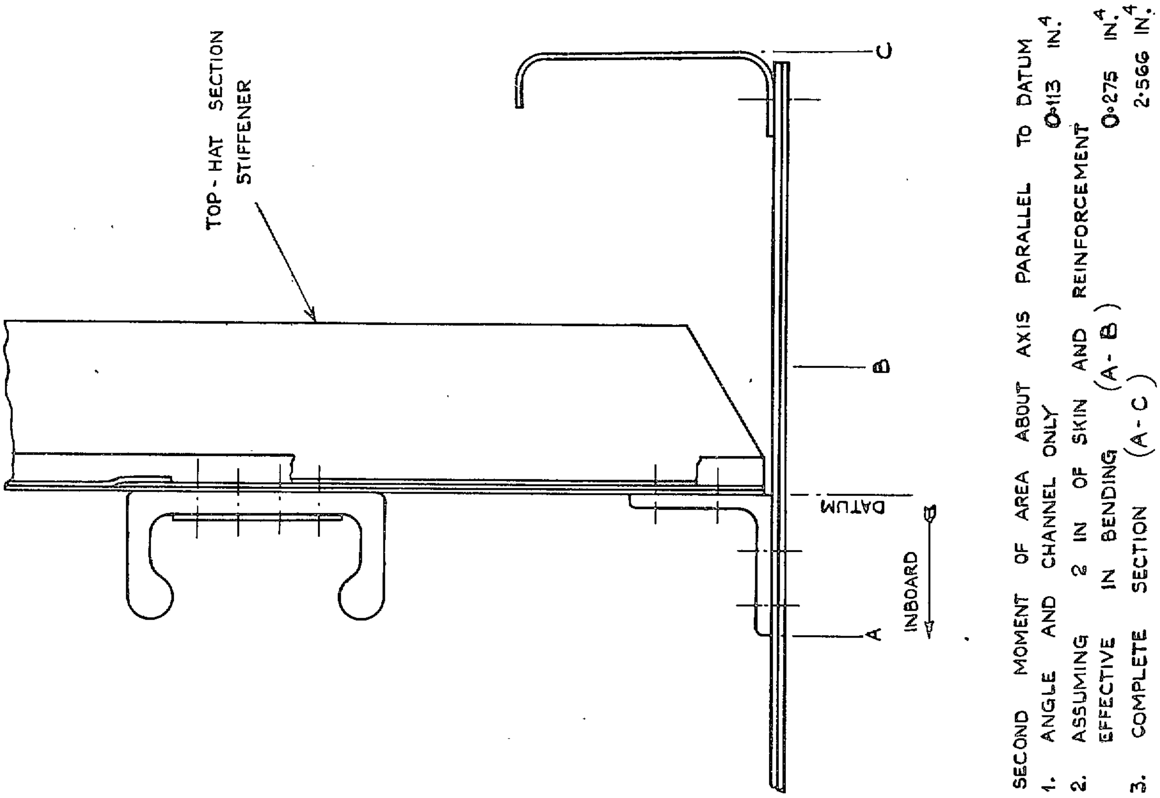

FIG. 4. Cross-section of chordwise rib at inboard edge of opening.

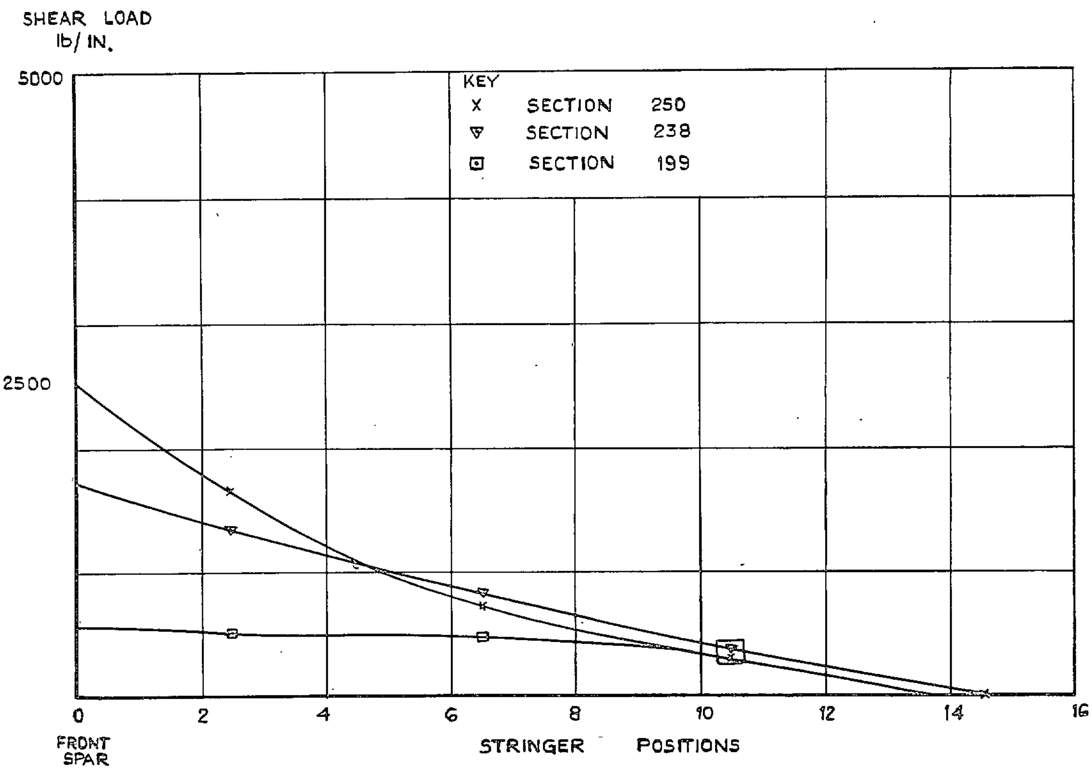

FIG. 5. Unmodified wing—chordwise distribution of measured shear loads.

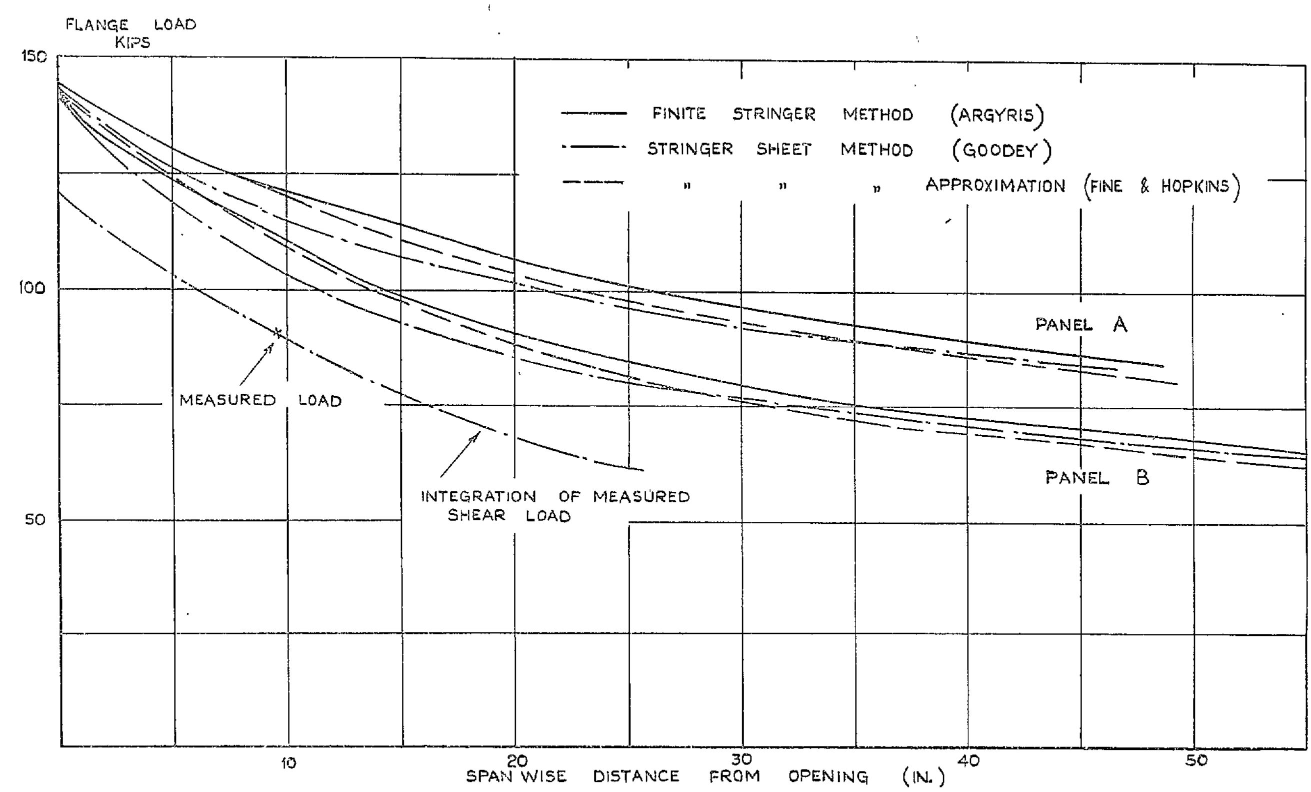

FIG. 6. Unmodified wing flange loads.

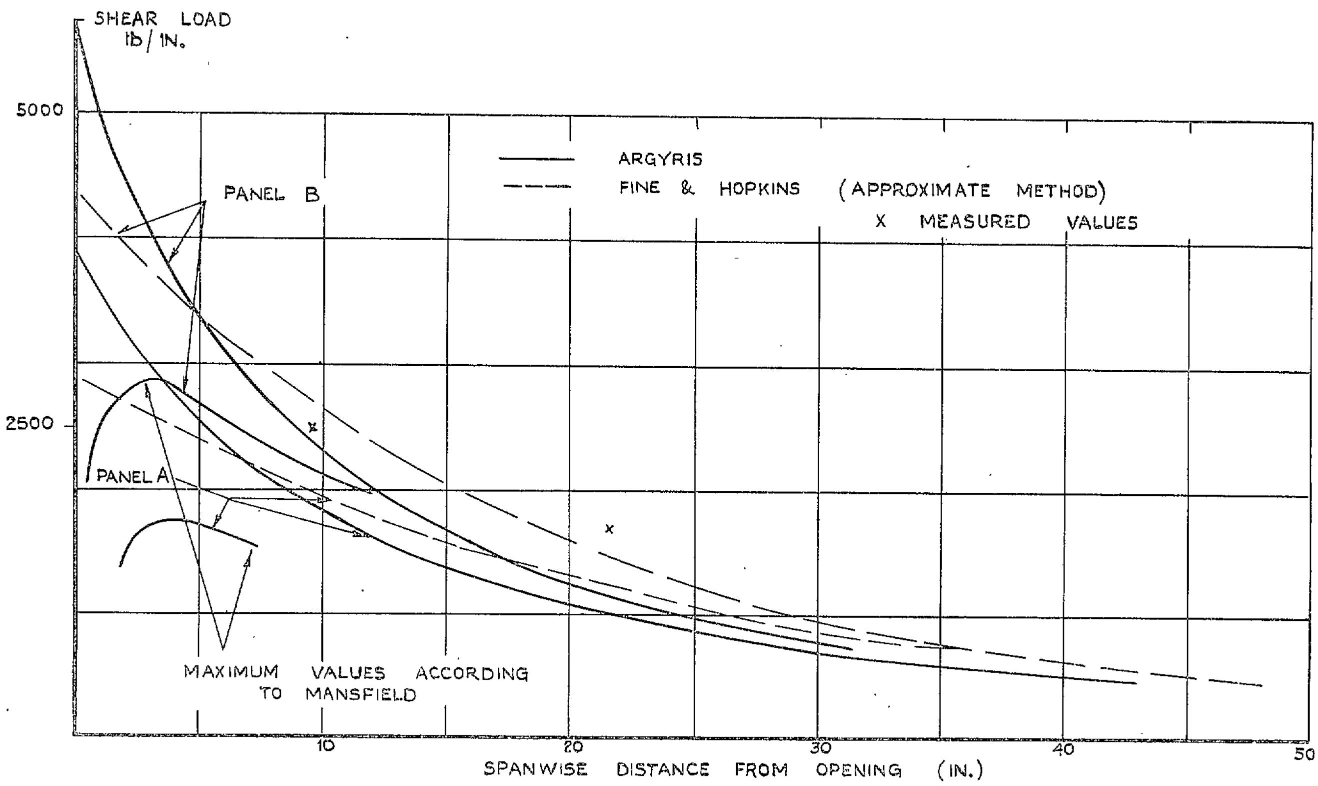

FIG. 7. Unmodified wing—shear load at front spar flange.

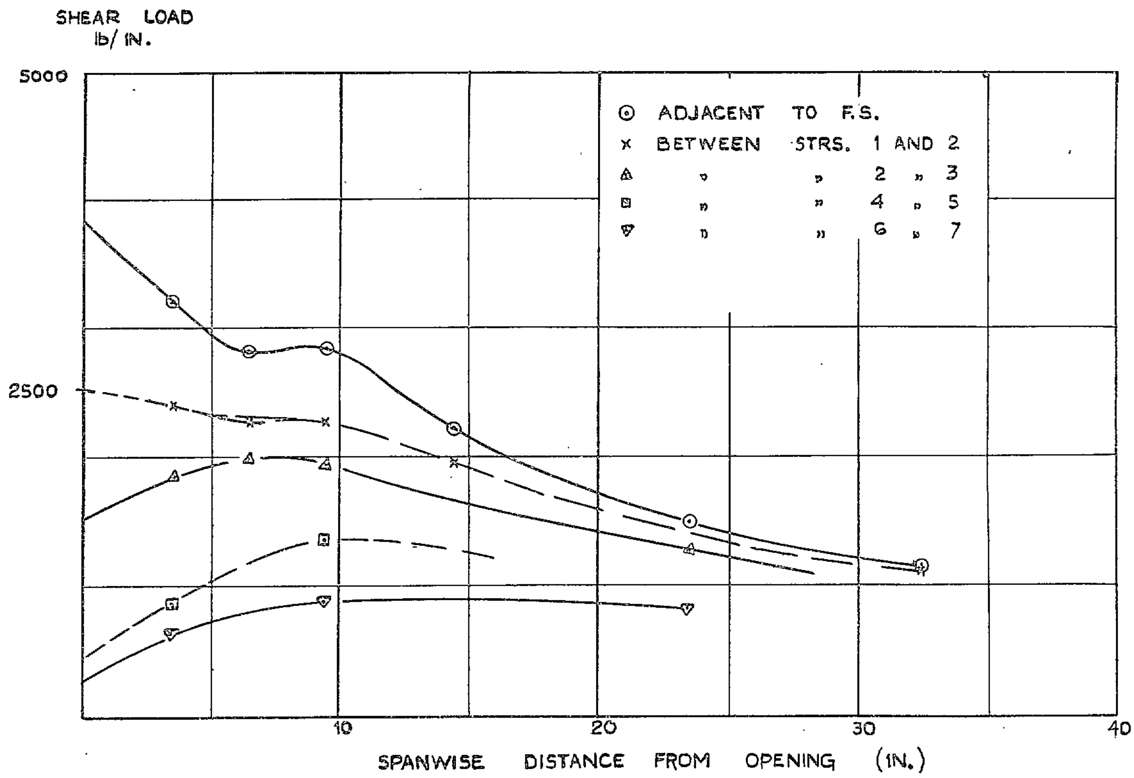

FIG. 8. Modified wing—spanwise distribution of measured shear loads.

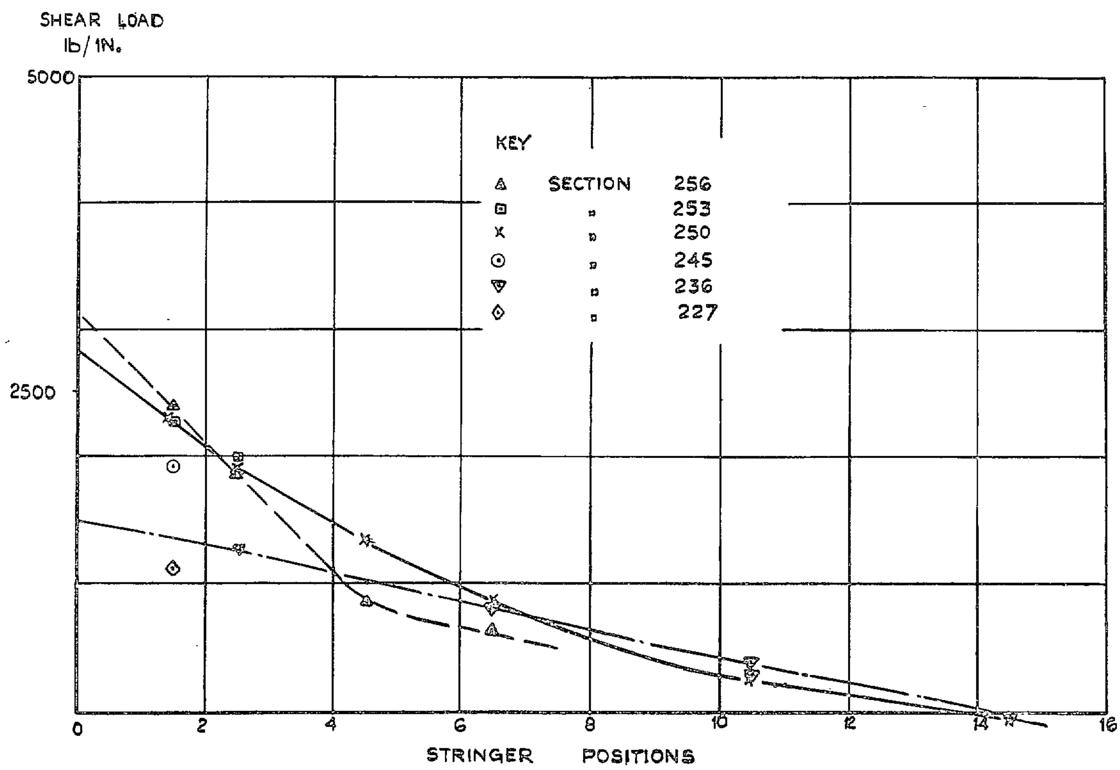

FIG. 9. Modified wing—chordwise distribution of measured shear loads.

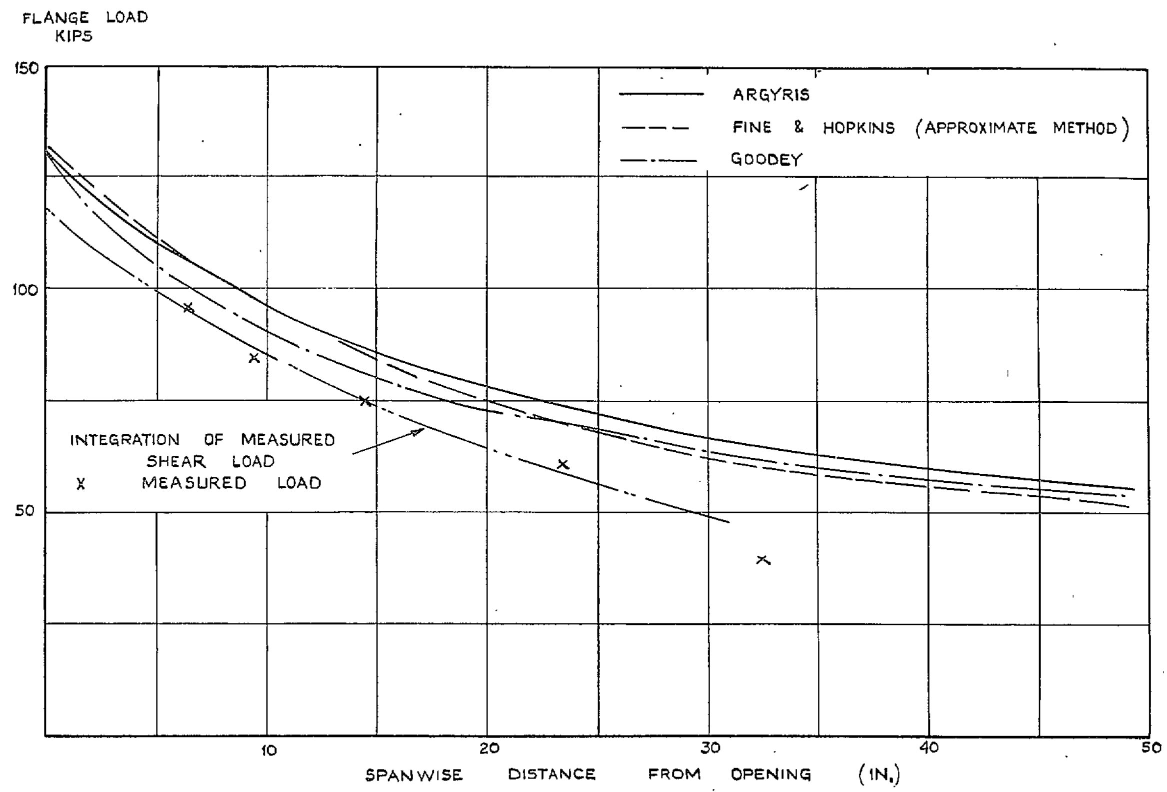

FIG. 10. Modified wing—flange loads.

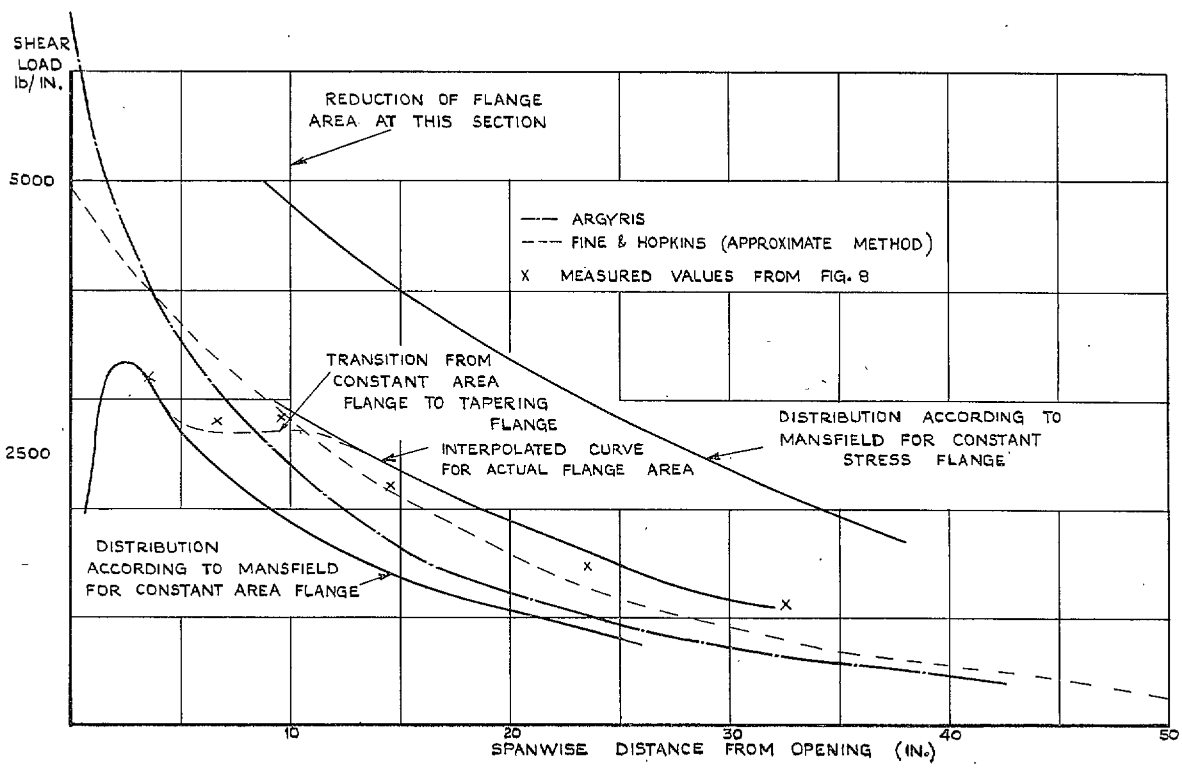

FIG. 11. Modified wing—shear load at front spar flange.

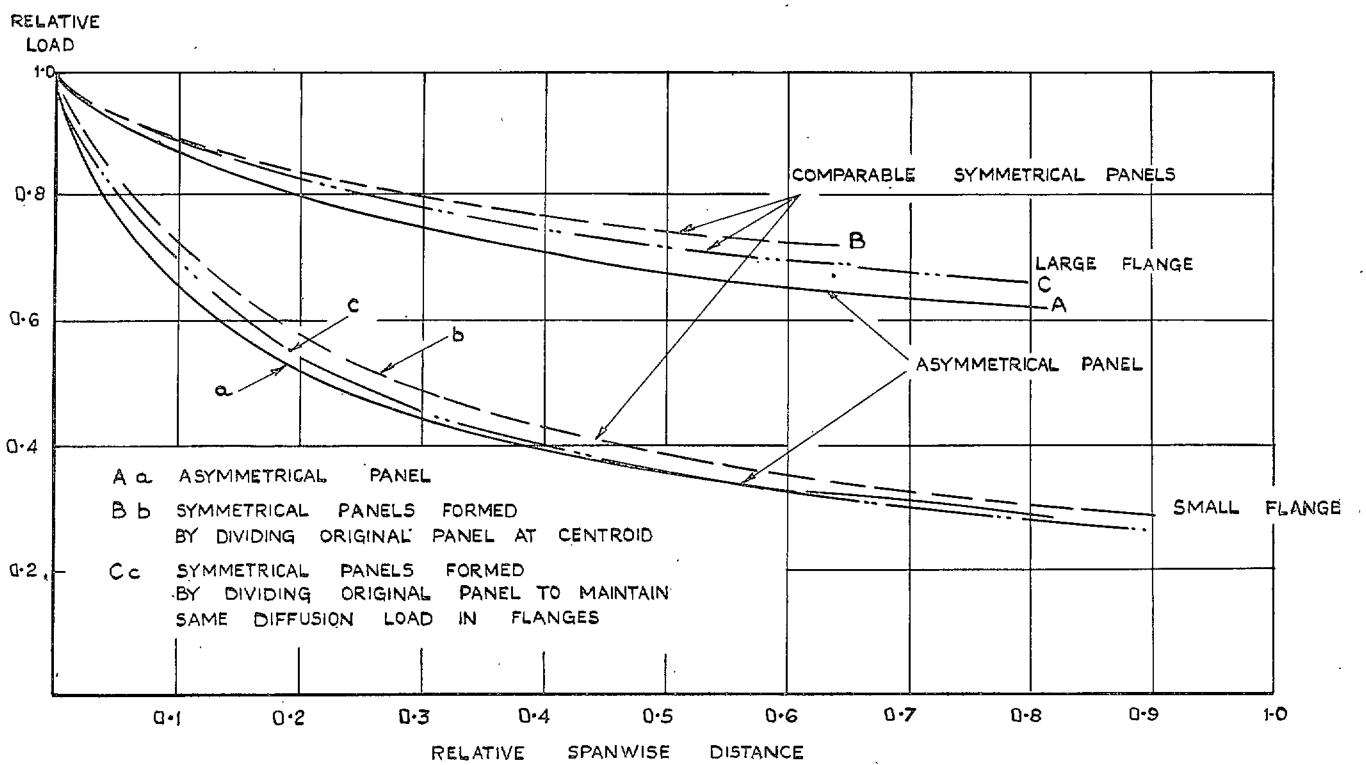

FIG. 12. Flange loads for asymmetrical and comparable symmetrical panels.

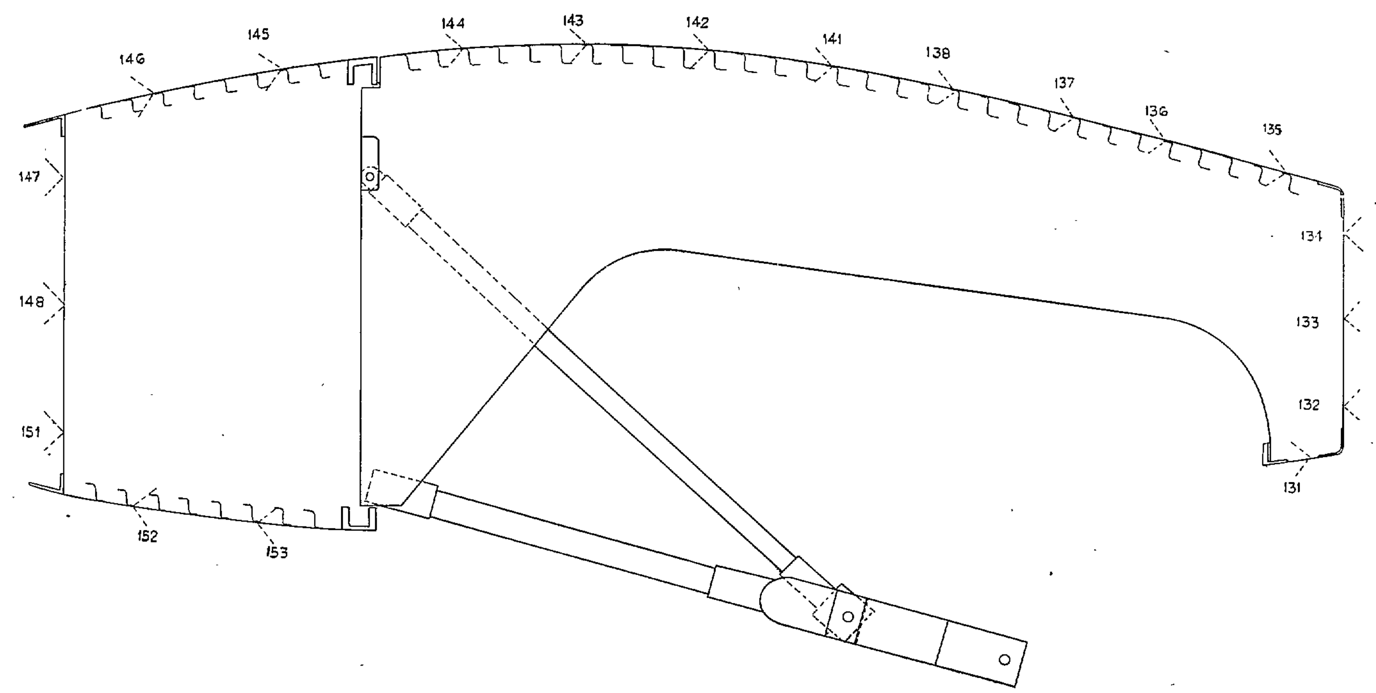

FIG. 13a. Strain gauge positions at Section 270.

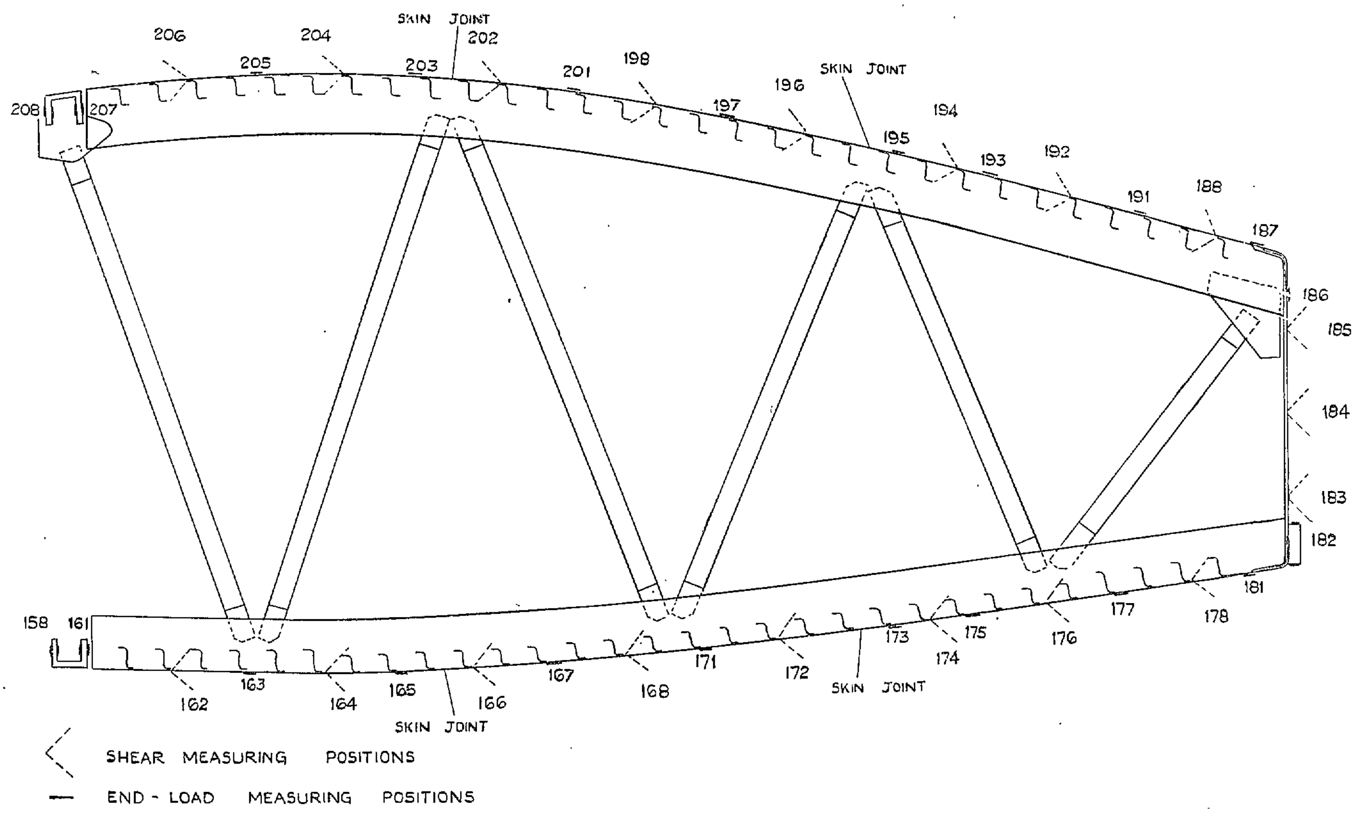

FIG. 13b. Strain gauge positions at Section 250.

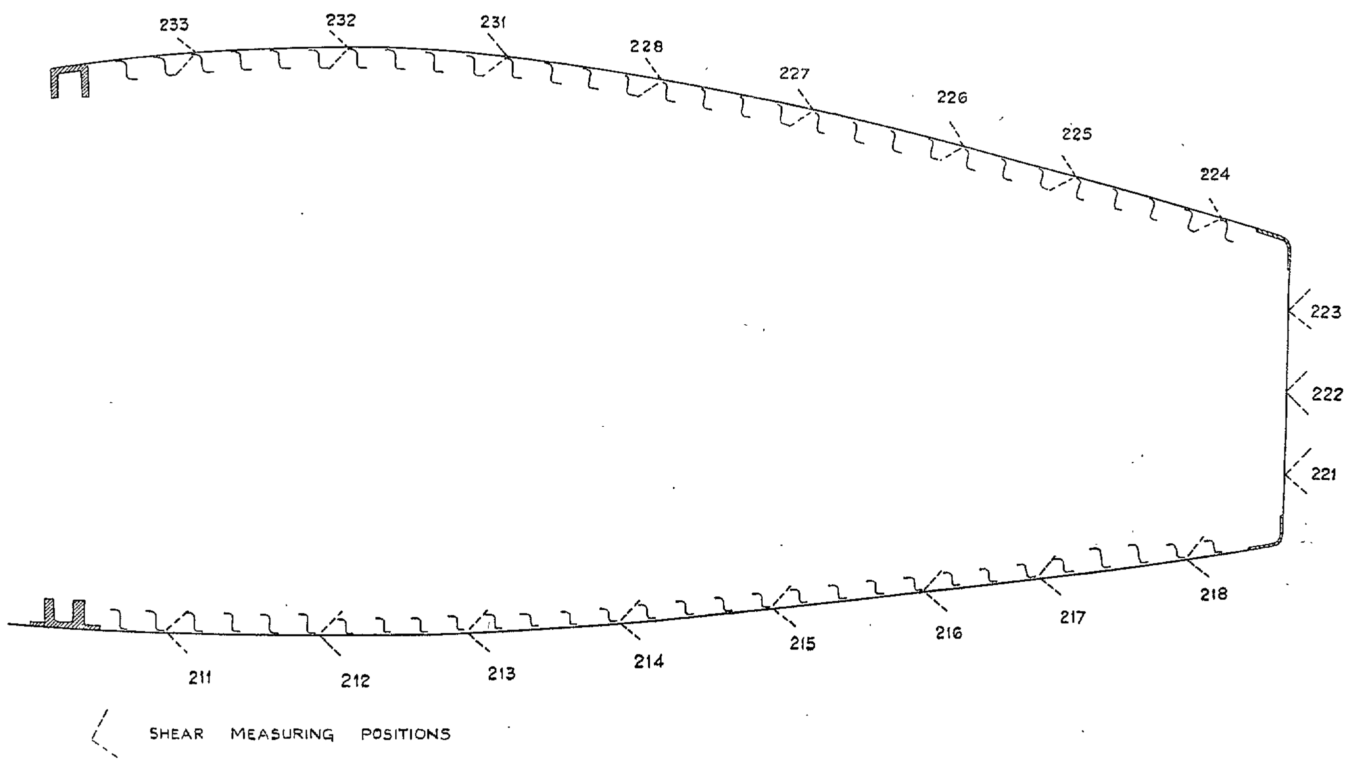

FIG. 13c. Strain gauge positions at Section 238.

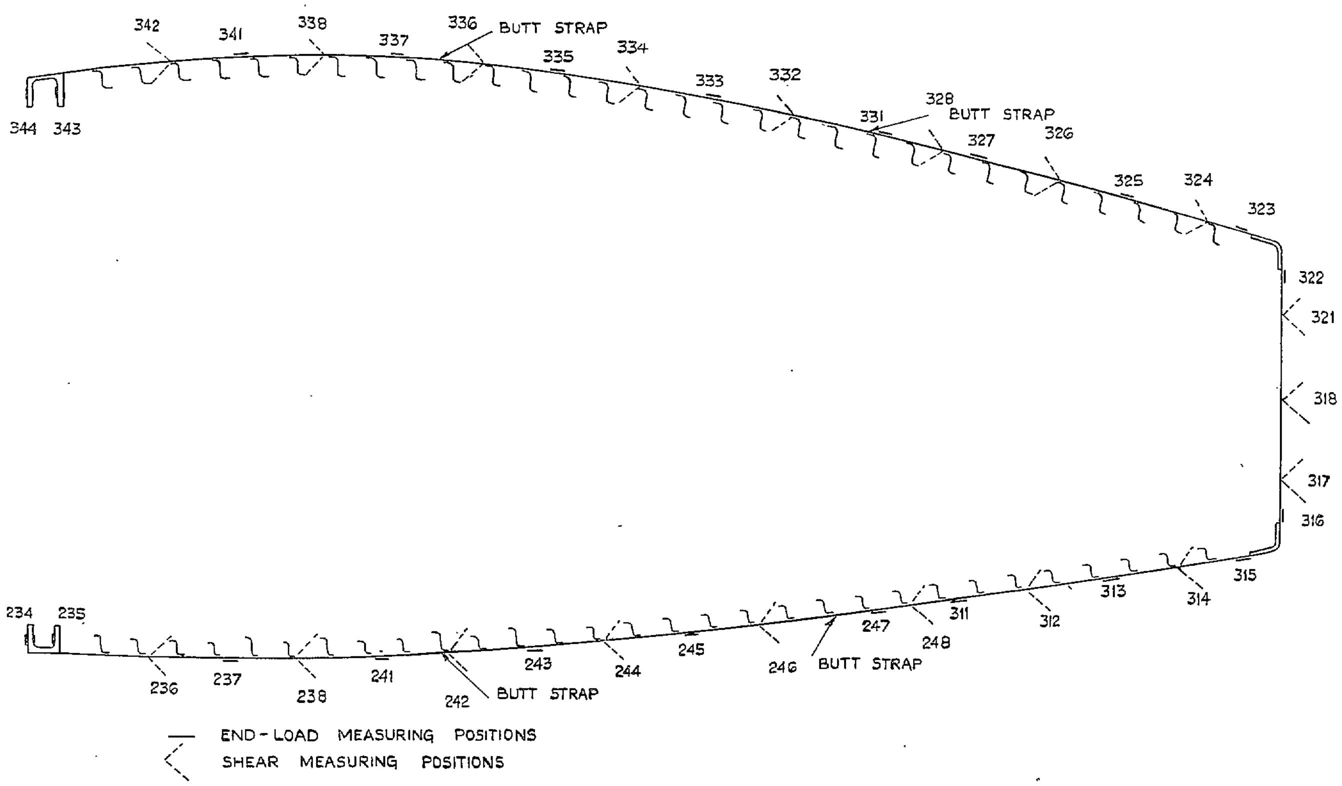

FIG. 14a. Strain gauge positions at Section 199.

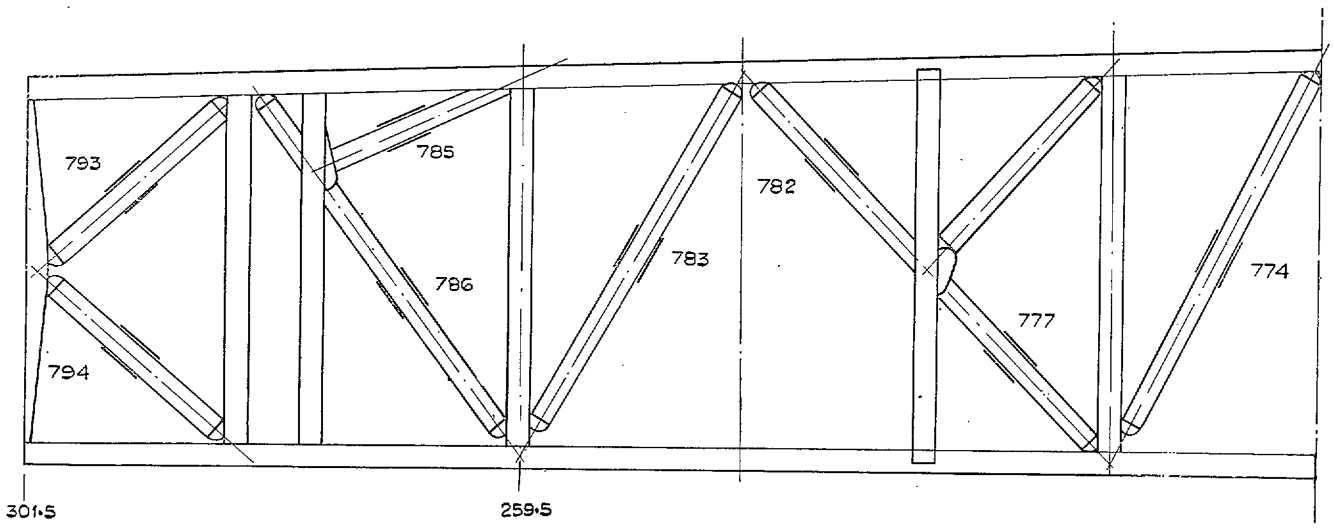

FIG. 14b. Strain gauge positions on front spar tubes.

(51765) Wt. 15/680 . K.5 7/52 Hw.

PRINTED IN GREAT BRITAIN

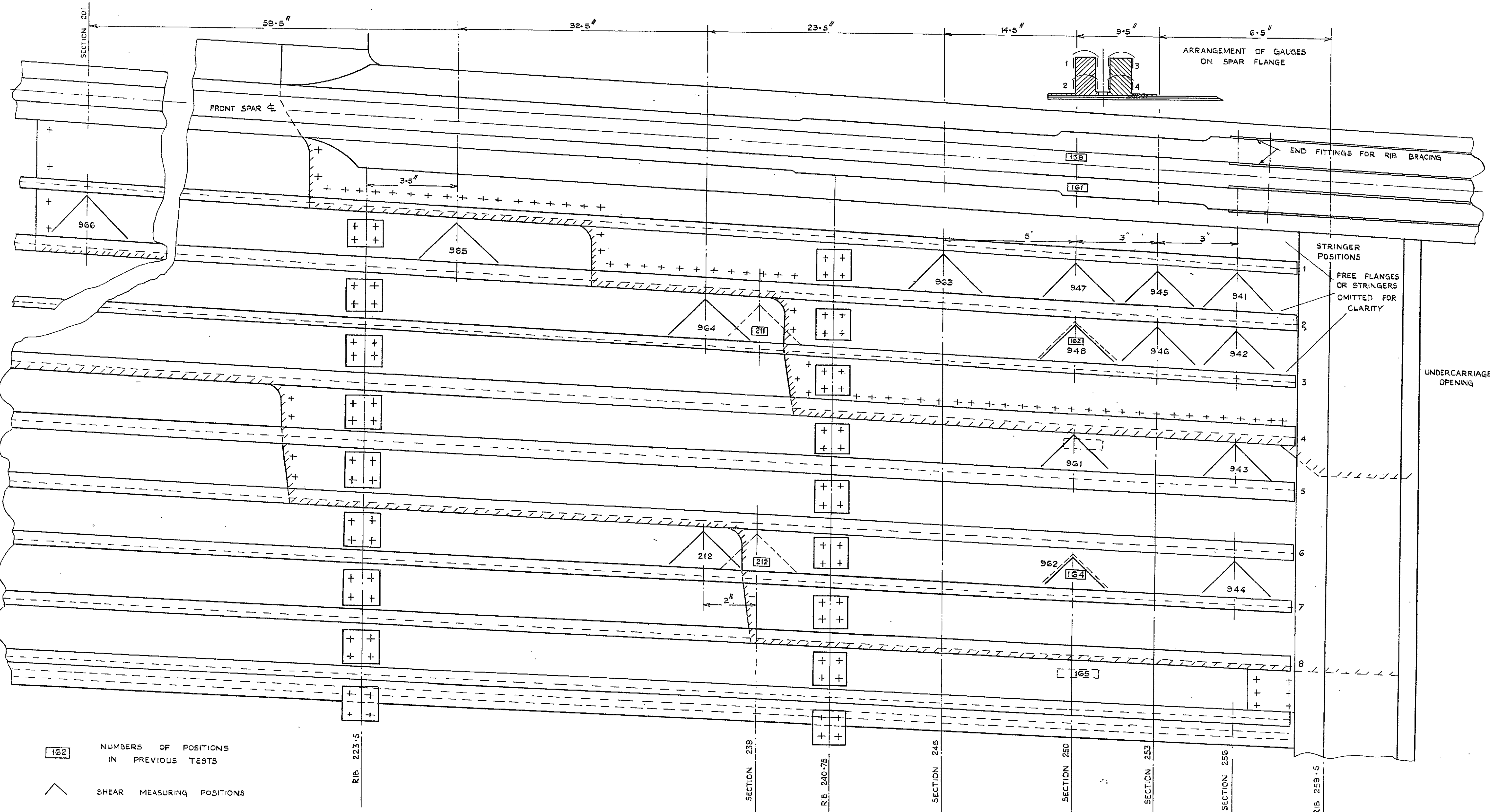

FIG. 15. STRAIN GAUGE POSITIONS IN FINAL TEST.

FIG. 15.

4600-15-680-1 M-6/52. (M.F.P.)

R. & M. No. 2664
(11,731)
A.R.C. Technical Report

Publications of the Aeronautical Research Council

ANNUAL TECHNICAL REPORTS OF THE AERONAUTICAL RESEARCH COUNCIL (BOUND VOLUMES)—

1934–35 Vol. I. Aerodynamics. *Out of print.*
Vol. II. Seaplanes, Structures, Engines, Materials, etc. 40*s*. (40*s*. 8*d*.)

1935–36 Vol. I. Aerodynamics. 30*s*. (30*s*. 7*d*.)
Vol. II. Structures, Flutter, Engines, Seaplanes, etc. 30*s*. (30*s*. 7*d*.)

1936 Vol. I. Aerodynamics General, Performance, Airscrews, Flutter and Spinning. 40*s*. (40*s*. 9*d*.)
Vol. II. Stability and Control, Structures, Seaplanes, Engines, etc. 50*s*. (50*s*. 10*d*.)

1937 Vol. I. Aerodynamics General, Performance, Airscrews, Flutter and Spinning. 40*s*. (40*s*. 10*d*.)
Vol. II. Stability and Control, Structures, Seaplanes, Engines, etc. 60*s*. (61*s*.)

1938 Vol. I. Aerodynamics General, Performance, Airscrews. 50*s*. (51*s*.)
Vol. II. Stability and Control, Flutter, Structures, Seaplanes, Wind Tunnels, Materials. 30*s*. (30*s*. 9*d*.)

1939 Vol. I. Aerodynamics General, Performance, Airscrews, Engines. 50*s*. (50*s*. 11*d*.)
Vol. II. Stability and Control, Flutter and Vibration, Instruments, Structures, Seaplanes, etc. 63*s*. (64*s*. 2*d*.)

1940 Aero and Hydrodynamics, Aerofoils, Airscrews, Engines, Flutter, Icing, Stability and Control, Structures, and a miscellaneous section. 50*s*. (51*s*.)

Certain other reports proper to the 1940 volume will subsequently be included in a separate volume.

ANNUAL REPORTS OF THE AERONAUTICAL RESEARCH COUNCIL—

1933–34	1*s*. 6*d*. (1*s*. 8*d*.)
1934–35	1*s*. 6*d*. (1*s*. 8*d*.)
April 1, 1935 to December 31, 1936.	4*s*. (4*s*. 4*d*.)
1937	2*s*. (2*s*. 2*d*.)
1938	1*s*. 6*d*. (1*s*. 8*d*.)
1939–48	3*s*. (3*s*. 2*d*.)

INDEX TO ALL REPORTS AND MEMORANDA PUBLISHED IN THE ANNUAL TECHNICAL REPORTS, AND SEPARATELY—

April, 1950 R. & M. No. 2600. 2*s*. 6*d*. (2*s*. 7½*d*.)

INDEXES TO THE TECHNICAL REPORTS OF THE AERONAUTICAL RESEARCH COUNCIL—

December 1, 1936 — June 30, 1939.	R. & M. No. 1850.	1*s*. 3*d*. (1*s*. 4½*d*.)
July 1, 1939 — June 30, 1945.	R. & M. No. 1950.	1*s*. (1*s*. 1½*d*.)
July 1, 1945 — June 30, 1946.	R. & M. No. 2050.	1*s*. (1*s*. 1½*d*.)
July 1, 1946 — December 31, 1946.	R. & M. No. 2150.	1*s*. 3*d*. (1*s*. 4½*d*.)
January 1, 1947 — June 30, 1947.	R. & M. No. 2250.	1*s*. 3*d*. (1*s*. 4½*d*.)

Prices in brackets include postage.

Obtainable from

HER MAJESTY'S STATIONERY OFFICE

York House, Kingsway, LONDON, W.C.2 423 Oxford Street, LONDON, W.1
P.O. Box 569, LONDON, S.E.1
13a Castle Street, EDINBURGH, 2 1 St. Andrew's Crescent, CARDIFF
39 King Street, MANCHESTER, 2 Tower Lane, BRISTOL, 1
2 Edmund Street, BIRMINGHAM, 3 80 Chichester Street, BELFAST

or through any bookseller.

S.O. Code No. 23-2664